Applied Clay Science 135 (2017) 394–404

Contents lists available at ScienceDirect

Applied Clay Science

journal homepage: www.elsevier.com/locate/clay

Research paper

Effect of chemical modification of palygorskite and sepiolite by 3-aminopropyltriethoxisilane on adsorption of cationic and anionic dyes

Maisa A. Moreira [a], Katia J. Ciuffi [a], Vicente Rives [b], Miguel A. Vicente [b,*], Raquel Trujillano [b], Antonio Gil [c], Sophia A. Korili [c], Emerson H. de Faria [a,*]

[a] Universidade de Franca, Av. Dr. Armando Salles Oliveira, Parque Universitário, 201, 14404-600 Franca, SP, Brazil
[b] GIR-QUESCAT, Departamento de Química Inorgánica, Facultad de Ciencias Químicas, Universidad de Salamanca, Plaza de la Merced, S/N, 37008 Salamanca, Spain
[c] Departamento de Química Aplicada, Universidad Pública de Navarra, Campus de Arrosadía, E-31006 Pamplona, Spain

ARTICLE INFO

Article history:
Received 7 July 2016
Received in revised form 13 October 2016
Accepted 13 October 2016
Available online 19 October 2016

Keywords:
Clays
Chemical modification
Aminosilane
Adsorption of dyes

ABSTRACT

A study has been performed on the removal of representative cationic and anionic dyes, methylene blue and metanil yellow, from aqueous solutions using fibrous clay minerals grafted with amine groups using (3-aminopropyl)triethoxysilane as functionalizing agent. Parameters affecting dye uptake, including contact time and dye concentration, the desorption process, pH and the recovery of both the dyes and the adsorbents, were evaluated. The adsorption capacities were 49.48 and 47.03 mg/g for grafted palygorskite and 60.00 and 59.78 mg/g for grafted sepiolite, for methylene blue and metanil yellow dyes, respectively. Adsorption of the anionic dye was enhanced by the grafting process. Grafted clay mineral adsorbents proved to be efficient to remove the contaminants from a real wastewater from textile industry within 30 min. Both adsorbents showed good reusability and the maximum adsorption capacity was maintained stable after a 2-cycle test. Thus, hybrid adsorbents based on fibrous clay minerals can efficiently be applied in adsorption/desorption cycles for removal of dyes.

1. Introduction

Water pollution, mainly due to industrial processes, is one of the most serious environmental problems in modern society (Anandkumar and Mandal, 2011). Many industries, such as paper and pulp, cosmetics, paints and pigments, plastics, leather tanning and textile, generate huge amounts of *colored effluents* which contain considerable amounts of toxic substances (Ozer et al., 2007; Demirbas et al., 2008).

Palygorskite (*Pal*) and sepiolite (*Sep*) are fibrous clay minerals whose basic structure can be described as 2:1 ribbons laterally linked to each other by single basal oxygens (Galán and Singer, 2011). The structure of Pal is similar to that of Sep except that a shorter *b* dimension incorporates only two linked pyroxene-like chains in the ribbon width, instead of three for Sep. This unique structural arrangement results in a large specific surface area (higher than 200 m^2/g) and good adsorption capacity for several organic compounds (Önal and Sarikaya, 2009; Galán and Singer, 2011).

Grafting of organo-alkoxides containing various groups, such as amine, mercapto or chlorine, among others, on different matrices has been recently reported by several authors, e.g., on silica (Linneen et al., 2014; Tiozzo et al., 2014), alumina (Afkhami et al., 2011; Saha and Sarkar, 2012), or zeolites (Bezerra et al., 2014), as well as layered (Tonlé et al., 2007; Önal and Sarikaya, 2009; Letaief et al., 2011; Wayde et al., 2011) or fibrous clay minerals (Letaief et al., 2011). The functionalizing molecules promote specific properties of the inorganic matrices providing or enhancing interesting properties to the grafted materials, making them potentially applicable in environmental remediation of various pollutants such as dyes, pesticides, heavy metals and drugs.

As indicated above, dyes are released into effluents from textile, leather, shoes polish, wood stain, paper, food and cosmetic industries, among others (Ozer et al., 2007; Demirbas et al., 2008; Anandkumar and Mandal, 2011). Metanil yellow, MY (monosodium salt of 3-(4-anilinophenylazo)benzenesulfonic acid, Fig. S1) is manufactured for textile industries and other purposes, and although it is non-permitted for coloration of food, it is extensively used in India and other countries (Nagaraja and Desirajut, 1993; El–Rehim et al., 2012). The environmental damage due to synthetic azo dyes is of increasing concern due to their serious health effects on animals and human beings. MY has carcinogenic effects due to the changes that can promote in the DNA synthesis (Nagaraja and Desirajut, 1993; Jain et al., 2003). Methylene blue, MB (3,7-bis(dimethylamino)-phenothiazin-5-ium chloride, Fig. S1), has practical application in the textile industry and has been used in a

* Corresponding authors.
E-mail addresses: mavicente@usal.es (M.A. Vicente), emerson.faria@unifran.edu.br (E.H. de Faria).

http://dx.doi.org/10.1016/j.clay.2016.10.022
0169-1317/

large number of studies as model of cationic dyes (Jain et al., 2003; Ozer et al., 2007; Demirbas et al., 2008; Anandkumar and Mandal, 2011).

Several methods for treatment of dye-containing wastewater have been developed recently, including adsorption on various matrices (Jain et al., 2003; Ozer et al., 2007; Demirbas et al., 2008; Anandkumar and Mandal, 2011), advanced oxidation processes (AOP) such as Fenton and photo-Fenton (Sahoo and Gupta, 2012; Barbosa et al., 2015) or electrochemical treatments (Gupta et al., 2007), among others. Removal and recovery of dyes from solutions by a simple and versatile adsorption method is certainly an emerging field of research, because adsorption is a clean operation and can completely remove the dyes even from dilute solutions (Ozer et al., 2007; Demirbas et al., 2008; Anandkumar and Mandal, 2011; Galán and Singer, 2011). The most commonly used adsorbent is activated carbon, due to its very high specific surface area and large amount of adsorption sites on the surface. However, commercially available activated carbons are very expensive. Alternatively, modification of natural clay minerals by organic groups can improve their adsorption capacity and make them suitable for the adsorption of various compounds. In fact, several issues related to the preparation and application of hybrid materials based on fibrous clay minerals have been addressed, as the use of long- or short-chain organic compounds containing different functional groups, thus tailoring the hydrophobicity, the affinity of the functional groups for different organic and inorganic pollutants, the mechanism of partitioning at the solid/solution interface, etc. (Frost and Mendelovici, 2006; Frost et al., 2010; Galán and Singer, 2011; Xue et al., 2011; Ruiz–Hitzky et al., 2013; Matusik and Wścisło, 2014).

The adsorption of cationic and anionic species on one single matrix has attracted a great interest in recent years, and hybrid compounds are good candidates for this purpose, as they show high versatility and usability, as well as increased performance by combining the properties of the matrix with the functionality of the organic compound. Taking into account the importance of environmental studies based in natural clay minerals, the adsorption of cationic and anionic dyes (methylene blue, MB, and metanil yellow, MY) on two fibrous clay minerals, sepiolite and palygorskite, organofunctionalized with the alkoxide 3-aminopropyltrietoxysilane (APTES), has been studied in the present work. Our main purpose was to verify and to understand the effect of chemical modification of these two fibrous natural clay minerals (palygorskite and sepiolite) with aminosilanes on their adsorption properties.

2. Experimental

2.1. Materials

The adsorbates MB (C.I.: 52015, chemical formula: $C_{16}H_{18}ClN_3S.xH_2O$, MW: 333.6 g/mol, maximum absorbance λ = 665 nm) and MY (C.I.: 13065, chemical formula: $C_{18}H_{14}N_3NaO_3S$, MW: 375.38 g/mol, maximum absorbance λ = 440 nm) were supplied by Sigma-Aldrich.

2.2. Purification of fibrous clay minerals

The fibrous clay minerals used in this work were palygorskite from Attapulgus, Georgia, USA (Clay Minerals Society), also known as attapulgite, and sepiolite from Vallecas, Madrid, Spain, commercially available as PANGEL, and kindly supplied by TOLSA, S.A. Both were purified according to the dispersion-decantation method (Bizaia et al., 2009), obtaining very pure clay minerals (Fig. 1). In the formulation of the samples, purified palygorskite and sepiolite are abbreviated as *Pal* and *Sep*, respectively.

2.3. Synthesis of the amino-hybrid clay minerals

The hybrid organic-inorganic materials were obtained by keeping a mass of 10.0 g of the precursor (Pal or Sep) in the presence of 50.0 cm^3 of (3-aminopropyl)triethoxysilane (APTES) for 48 h at 180 °C and under nitrogen atmosphere (without using any solvent, as APTES is a liquid). So, the clay mineral:APTES mass/volume ratio used was 1:5. The resulting materials were washed twice with toluene, then 5 times with ethanol and finally 5 times with water and oven-dried at 80 °C for 24 h; they were named as Pal-APTES and Sep-APTES, respectively.

2.4. Adsorption experiments

2.4.1. Kinetic studies

The adsorption kinetics was determined by analyzing the adsorptive uptake of the dyes from aqueous solutions at several time intervals. Volumes of 5.0 cm^3 of solutions of each dye with an initial concentration of 25 mg/dm^3 were poured in glass tubes and mixed with 0.05 g of each adsorbent, at room temperature, and with continuous magnetic stirring. At predetermined time intervals, between 0.1 and 60 min, the solid phase was separated by centrifugation at 3500 rpm. The dye concentration in the supernatant liquid was analyzed by UV–visible spectroscopy, using a Hewlett-Packard Model 8453 diode array spectrometer, determining the absorption at 665 nm for MB and 440 nm for MY, these being their respective maximum absorbance wavelengths. The amount of MB and MY adsorbed by the functionalized hybrid fibrous clay minerals was calculated by Eq. (1):

$$q_t = V \cdot (C_0 - C_t)/m \quad (1)$$

where q_t (mg/g) is the amount of dye adsorbed at time t (min), C_0 (mg/dm^3) is the initial concentration of the dye in the solution, C_t

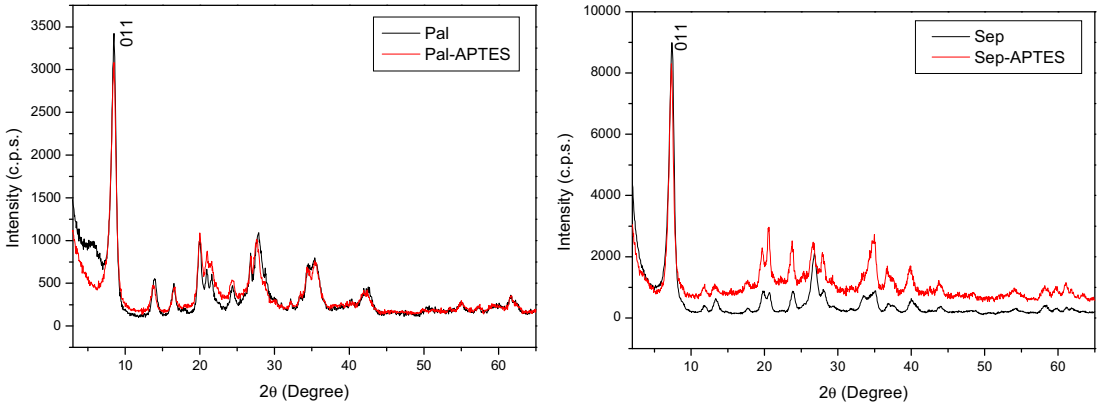

Fig. 1. X-ray powder diffraction patterns of parent clay minerals and of the APTES-functionalized solids.

(mg/dm^3) is the dye concentration in the solution at time t, V (dm^3) is the volume of the solution, and m (g) is the mass of adsorbent used.

2.4.2. Adsorption equilibrium studies

Adsorption equilibrium experiments were carried out in glass vials, by shaking a known amount of the adsorbent, typically 0.05 g, with 5.0 cm^3 of dye solution at given concentration values, in the range of 1 to 600 mg/dm^3. The vials containing the dye solutions and the adsorbent were shaken for 30 min at 25 °C, and the solid phase was then separated from the supernatant by centrifugation at 3500 rpm. The concentration of the dyes in the solution was immediately determined by UV–vis spectroscopy as described above, and the amount of adsorbed dyes were calculated using Eq. (2), where q_e (mg/g) is the amount of dye adsorbed at time t (min), C_0 and C_e (mg/dm^3) are the initial and equilibrium dye concentrations, V (dm^3) is the volume of the solution, and m (g) is the mass of adsorbent employed.

$$q_e = V \cdot (C_0 - C_e)/m \quad (2)$$

2.4.3. Desorption experiments

The solids obtained from equilibrium studies, that is, containing MB or MY adsorbed on Pal-APTES or Sep-APTES, were magnetically stirred for 1440 min at 25 °C using the following solutions: water, sodium chloride (0.1 mol/dm^3) in water, or sodium chloride (0.1 mol/dm^3) in methanol. After contacting with these extraction solutions, the samples were centrifuged at 3500 rpm and the supernatant liquid analyzed by UV–vis spectroscopy. All experiments were conducted in duplicate. The amounts of desorbed dye were calculated as percentage of the amounts adsorbed during the adsorption equilibrium process.

2.4.4. Reuse experiments

To evaluate the stability and reusability of the adsorbents, the solids were recovered after the desorption experiments described in the previous section, and reused as adsorbents, under the same conditions as for the equilibrium experiments (0.05 g of recovered adsorbent, 5.0 cm^3 of 600 mg/dm^3 dye solution, 30 min, 25 °C). After adsorption, the solids were centrifuged at 3500 rpm and the supernatant liquid analyzed by UV–vis spectroscopy. The yield of adsorption was compared to the first use of each adsorbent.

2.4.5. pH effect

The effect of pH on the adsorption of the dyes was studied in the range of 2–10. The evaluation was based on the last point of the equilibrium isotherms, fixing the parameters of adsorption contact time and concentration on the basis of kinetic and equilibrium studies. The initial dye (MB and MY) concentration was 600 mg/dm^3 and the pH was adjusted adding 0.1 mol/dm^3 NaOH or HCl solutions.

2.4.6. Real dyestuff wastewater adsorption proof

10.0 cm^3 of two real wastewater samples A (before biological treatment) and B (after biological treatment) were initially centrifuged at 3500 rpm for 10 min to remove the existing solid particles and fibers from textile residues. Then, a portion of 5.0 cm^3 of each one of the real wastewater samples was kept in contact with 50.0 mg of the hybrid adsorbents Pal-APTES or Sep-APTES using vial glass flasks and maintained under magnetic stirring for 60 min, at 25 °C. The specific conditions used were based on the previous kinetic and equilibrium studies of the dyes used as models. The amount of contaminant adsorbed was quantified by UV–vis absorption spectroscopy, using the band at 256 nm. In the specific case of wastewater A, dilution of the sample before quantification of the amount adsorbed was required; 1.0 cm^3 of the sample was diluted to 25.0 cm^3 with distilled water.

2.5. Characterization of the solids

The X-ray diffractograms of the solids were acquired in a Siemens D-500 diffractometer operating at 40 kV and 30 mA (1200 W), using filtered Cu Kα radiation and varying the 2θ angle from 2° to 65°. All the analyses were carried out at a scan speed of 2°/min.

The thermal analyses were carried out in a TA Instrument SDT Q600 Simultaneous DTA-TGA thermal analyzer, at temperatures ranging from 25 to 900 °C, at a heating rate of 10 °C/min and air flow of 100 cm^3/min.

The FTIR spectra were recorded in a Perkin-Elmer Spectrum One spectrometer, using the KBr pellet technique. The spectra were recorded between 400 and 4000 cm^{-1}, with a nominal resolution of 4 cm^{-1}.

Scanning electron microscopy (SEM) of the materials was performed on a Zeiss DSM 960 digital scanning microscope at Servicio General de Microscopía Electrónica (NUCLEUS, Universidad de Salamanca, Spain). The samples were previously coated with a thin gold layer by evaporation using a Bio-Rad ES100 SEN coating system.

Textural analyses were carried out by nitrogen adsorption at −196 °C using a static volumetric apparatus (Micromeritics ASAP 2020 adsorption analyzer). Prior to analysis, 0.2 g of sample was degassed for 24 h at 150 °C at a pressure lower than 0.133 Pa. The specific surface area was obtained by the BET method (S_{BET}), and the total pore volume was calculated from the amount of nitrogen adsorbed at a relative pressure of 0.95.

The pH point of zero charge (pH_{PZC}) was determined by using 12 flasks with 20 mg of each adsorbent, adding aliquots of 5 cm^3 of 0.1 mol/dm^3 NaCl at different initial pH between 1 and 12. Solutions of HCl (0.1 mol/dm^3) or NaOH (0.1 mol/dm^3) were used to change the pH. The pH was measured after shaking the suspensions for 24 h at room temperature. The pH_{PZC} value, determined by plotting the initial pH versus final pH, that was assigned to the zone where the pH did not change drastically, and did not depend of the initial pH, as the surface of the material acted as a buffer. All these analysis were made in triplicate.

3. Results and discussion

3.1. Characterization of the adsorbents

Pal and Sep contained low amount of impurities such as quartz and illite, which were completely removed during the purification process, yielding highly pure samples (Fig. 1). These purified clay minerals were grafted with APTES without further treatments. The assignment of the reflections for both clay minerals is given in Fig. S2.

The treatment with APTES did not give rise to significant changes in the solids. There were not changes in the basal distances, as these clay minerals are non-swellable, but a small decrease in the relative intensity of the 011 reflection suggested that bonding of APTES on the surface of the particles or within the channels induced a decrease of the stacking order. The other diffraction effects did not change with the treatment, indicating that grafting did not alter the structure of each individual layer. So, Sep and Pal structures were preserved after grafting with the aminosilane.

The thermal curves of Pal-APTES and Sep-APTES (Fig. 2) were similar to those reported for other grafted compounds (de Faria et al., 2009; Machado et al., 2013; Matusik and Wścisło, 2014), with the expected differences due to the specific nature of the clay minerals and the functionalizing molecule here used. Pal showed its first mass loss (9.4%) at 97 °C, associated to an endothermic peak, and attributed to the elimination of water molecules adsorbed on the clay mineral surface. Its second mass loss step, at 216 °C (2.3%), can be assigned to removal of zeolitic water from the channels and hydrogen-bonded to Al—OH or Si—O—Si groups in the fibrous structure. The third step was composed of two effects centered at 350 and 430 °C (9.7%), and was due to dehydroxylation of Pal.

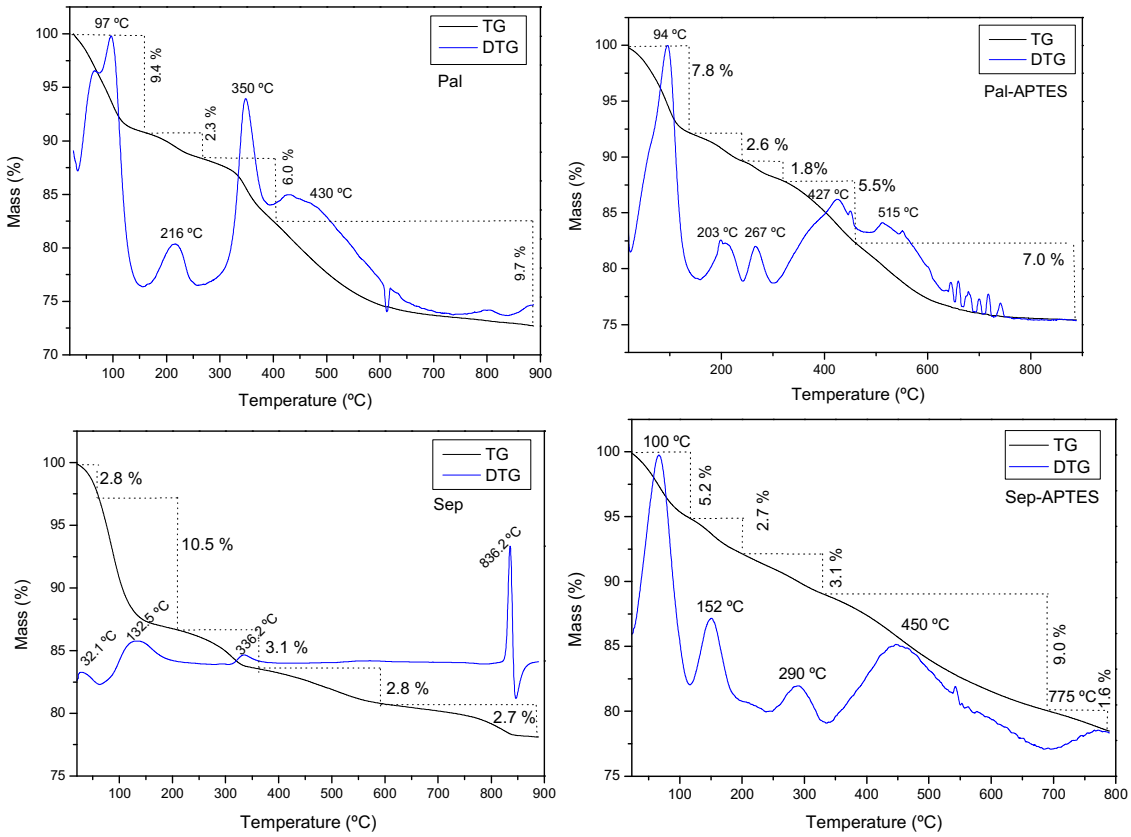

Fig. 2. Thermal analysis (TG/DTG) of Pal-APTES and Sep-APTES solids.

Grafting with APTES led to significant differences with respect to the original clay mineral. The first effect had a lower mass loss (7.9%), due to partial removal of surface adsorbed water during grafting. The mass loss associated to dehydroxylation of the clay mineral also decreased, in agreement with the participation of hydroxyl groups in the grafting process, while new mass losses at 350 and 430 °C were assigned to decomposition of grafted alkoxides. Sep-APTES had five mass loss steps. The first one, at 94 °C (7.8%), was assigned to water elimination. The second and third ones, at 203 (2.6%) and 267 °C (1.8%), were assigned to removal of zeolitic water and to the beginning of decomposition of APTES moieties, respectively. The fourth and fifth steps, at 427 (5.5%) and 515 °C (7.0%), were assigned to decomposition of organic matter from APTES, to the dehydroxylation of Sep and to removal of residual carbon content. The total mass loss was similar in both treated solids, close to 25%. The functionalizing molecules were not completely removed during heating, as a portion remained in the solid phase by forming amorphous silica from their Si atoms.

The amount of APTES fixed by unit cell of the clay minerals was calculated from the mass loss between 260 and 400 °C, considering the hydrolysis and condensation of one, two or three silanol groups onto the fibrous clay minerals; the average stoichiometries were Pal-APTES$_{0.249}$ and Sep-APTES$_{0.337}$ (formula of Pal referred to 4 Si atoms, and formula of Sep referred to 6 Si atoms). A plausible mechanism for the grafting reaction is proposed in Fig. S3.

The morphological changes induced by functionalization with the alkoxide molecule were evident in the SEM micrographs of the hybrid solids (Fig. 3). Natural clay minerals showed typical packed fibers (Neaman and Singer, 2000) or mats of tightly interwoven fibers (Cagatay, 1990; Frost et al., 2010), with variable thickness and length. These fibers had flat or straight shapes and were randomly oriented in aggregates. After grafting, larger aggregates with preferential orientation were formed, probably favored by the presence of amine groups that maintained the fibers together by hydrogen bonding between siloxane (Si—O—Si) or hydroxyl (Mg—OH) and amine (NH_2) groups. A similar behavior had been previously reported for grafting of various organosilanes into Pal or Sep (Cagatay, 1990; Frost et al., 2010; Neaman and Singer, 2000).

FTIR spectrum of Pal (Fig. 4) displayed the characteristic vibrations of the tetrahedral (Si—O—Si, 950–1250 cm^{-1}) and the octahedral (Al—Al—OH, 913 cm^{-1}; Al—Fe—OH, 865 cm^{-1} and Mg—Mg—OH, 650 cm^{-1}) sheets, with bands due to hydroxyls and water molecules at ca. 3200–3400 and 1652 cm^{-1}, respectively. The region between 1200 and 2000 cm^{-1} has been commonly used to identify organic molecules interacting with fibrous silicates (Frost and Mendelovici, 2006). The typical bands of amine groups were recorded at 1600 cm^{-1}, confirming the grafting on both fibrous clay minerals. The intensities of the bands in the high wavenumber region decreased as a result of the condensation of silanes with Mg—OH or Al—OH groups from the fibrous structures. In addition, new bands at 3479 and 3410 cm^{-1} in Pal-APTES were due to the amino groups. The absorption band at 2930 cm^{-1} corresponded to the C—H stretching vibration of APTES CH_2 groups. All these observations agreed with the grafting of APTES on the surface of Pal (Xue et al., 2011). Similar results were observed for grafted Sep.

The nitrogen adsorption–desorption isotherms for the natural and functionalized fibrous clay minerals (Fig. 5) belonged to Type II, with the presence of a H3-type hysteresis loop, typical of the mesoporous structure of these clay minerals (IUPAC Classification, Sing et al., 1985). The initial part of the isotherm was attributed to monolayer-multilayer adsorption, while H3-type loops evidenced that the solids did not exhibit any limiting adsorption at high relative pressure; this hysteresis loops are generally observed in adsorbents with aggregates of plate-like particles, such as fibrous or layered and also pillared clay minerals, giving rise to slit-shaped pores.

The presence of the alkoxide entities decreased in both cases the specific surface area (Table 1), probably because the surface-anchored

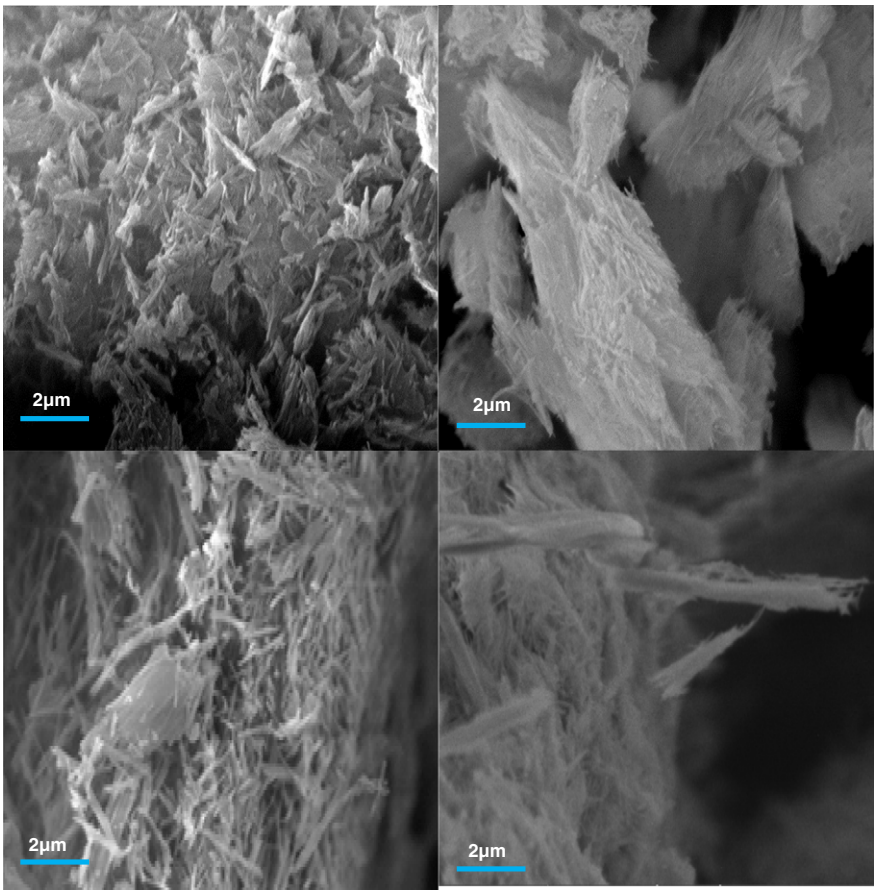

Fig. 3. SEM images of fibrous clay minerals: Pal (up) and Sep (down), natural (left) and modified with APTES (right).

APTES molecules partially blocked the nitrogen adsorption sites and the access of N_2 molecules to the channel pores. Comparing both clay minerals, Sep showed more promising properties, due to the higher specific surface area of the original solid, which was maintained in the grafted solid. Although functionalization decreased the specific surface area, the presence of amine groups could generate specific and selective adsorption sites. As Sep had higher surface area, the organic molecules may be more disperse, forming a wider framework that may not block the access of nitrogen molecules to the surface. The shape of the isotherms did not vary, suggesting only quantitative differences in porosity.

The APTES loading can be related to the decrease in specific surface area (Eq. (3)), assuming that N_2 surface coverage changed due to APTES grafting. However, it may be considered that APTES grafting could not only decrease the external surface, but also block the access to pore surface:

$$l = \frac{\left(S_{(BET)}grafted - S_{(BET)}nongrafted\right)}{APTES\ molec.area\ (m^2)} \times \frac{1}{N_A} \quad (3)$$

where l was the loading of APTES per gram of clay mineral, $S_{(BET)}$ *grafted* was the specific surface area after grafting with APTES, and $S_{(BET)}$ *nongrafted* the specific surface area of the purified fibrous clay mineral, before grafting. The values calculated (Table 1) are in agreement with the amount of APTES determined by thermal analysis (Fig. 2), and

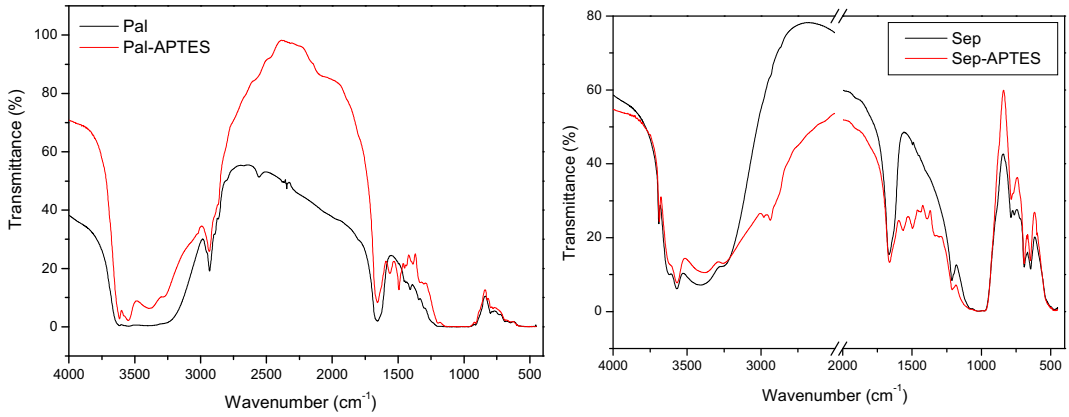

Fig. 4. FTIR absorption spectra of natural and grafted fibrous clay minerals.

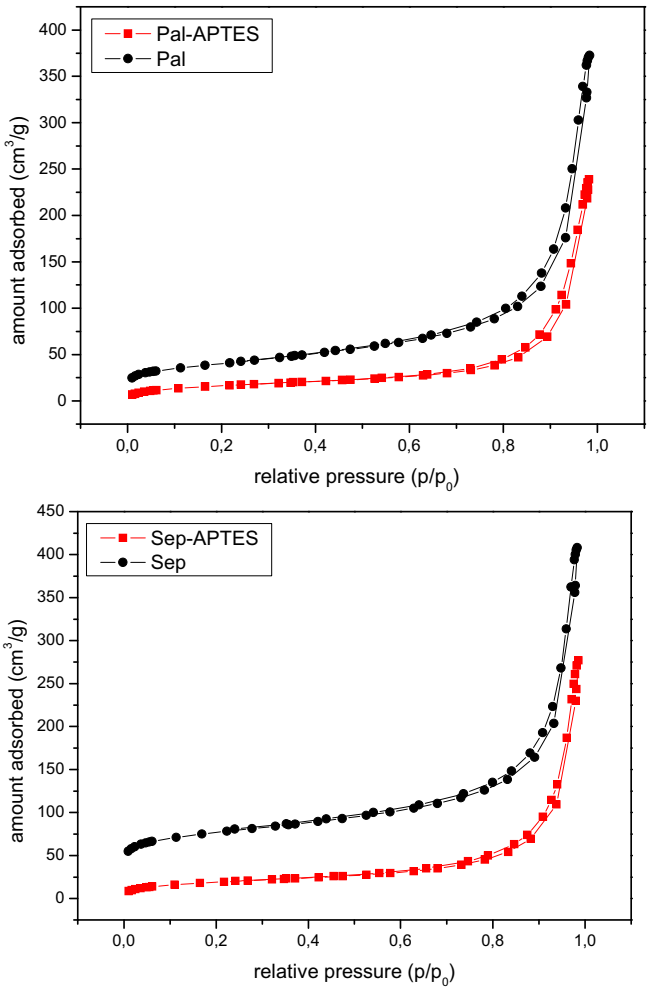

Fig. 5. Nitrogen adsorption–desorption isotherms (−196 °C) for original and functionalized palygorskite and sepiolite solids.

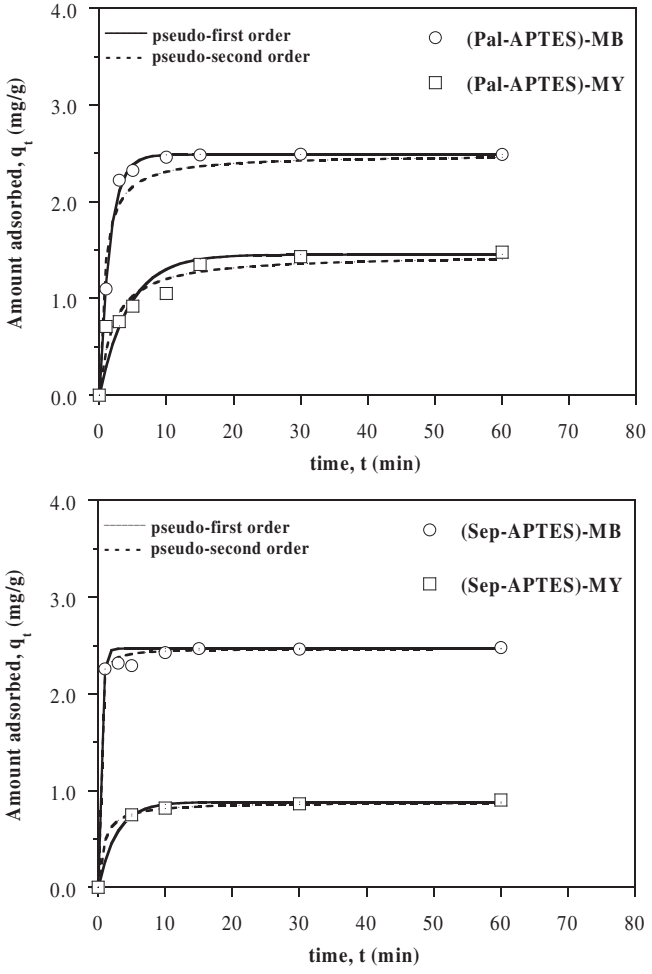

Fig. 6. Kinetic adsorption data of MB and MY using Pal-APTES and Sep-APTES as adsorbents.

suggested that most of APTES was on the external surface area of the clay mineral particles.

3.2. Adsorption experiments

3.2.1. Kinetic studies

To establish an optimum equilibrium time for the maximum uptake of dyes and to evaluate the kinetics of the process, the adsorption capacity of the adsorbents was measured as a function of contact time (Fig. 6). The time required to reach the maximum adsorption was 30 min, somewhat shorter for MB, and this contact time was used in the equilibrium adsorption experiments.

The knowledge of the adsorption kinetics is a fundamental point in adsorption studies, giving valuable evidences of the possibility of technological application of an adsorbent for a particular separation process.

Table 1
Specific surface area and pore volume of natural and functionalized palygorskite and sepiolite solids.

Sample	S_{BET} (m^2/g)	Pore volume (cm^3/g)	APTES loading (l) (mol/g)
Pal	139	0.576	–
Pal-APTES	59	0.369	$6.11 \cdot 10^{-5}$
Sep	245	0.631	–
Sep-APTES	67	0.429	$1.36 \cdot 10^{-4}$

The first-order and the pseudo-second-order kinetic models were used to elucidate the adsorption mechanism. The pseudo first-order kinetics model (Lagergren, 1898) is given by Eq. (4):

$$q_t = q_e \cdot [1 - \exp(-k_1 \cdot t)] \quad (4)$$

where q_e and q_t (mg/g) are the amounts of adsorbate adsorbed at equilibrium and at time t, respectively, and k_1 is the rate constant (min^{-1}) of the first-order model.

The pseudo-second-order kinetic model (Ho and Ofomaja, 2006) is expressed as:

$$q_t = \frac{k_2 \cdot q_e^2 \cdot t}{1 + k_2 \cdot q_e \cdot t} \quad (5)$$

where q_e is the maximum adsorption capacity (mg/g) for the pseudo-second-order adsorption, q_t is the amount of adsorbate (mg/g) adsorbed at time t (min) and k_2 is the rate constant of the pseudo-second-order adsorption (g^{-1}(mg·min)).

The kinetic parameters for the adsorption of MB and MY dyes on the fibrous clay minerals were calculated from the corresponding plots (Table 2). The data fitted much better to the pseudo second-order kinetic model than for the pseudo first-order one, evidencing that the adsorption process occurred by a chemisorption mechanism.

The fast removal of the dyes from solution, reaching the equilibrium in a rather short time, gave evidence that both functionalized fibrous clay minerals were efficient adsorbents. The simple forms of the kinetic

Table 2
Pseudo-first- and -second-order parameters for methylene blue (MB) and metanil yellow (MY) adsorption by modified clay minerals (C_0 = 25 mg/dm^3, T = 25 °C).

	MB		MY	
	Pal-APTES	Sep-APTES	Pal-APTES	Sep-APTES
First-order				
k_1 (1/min)	0.63	2.44	0.23	0.36
χ^2	0.020	0.057	0.25	0.0024
R	0.998	0.994	0.92	0.998
Second-order				
k_2 (g^{-1} mg·min)	0.52	3.40	0.32	1.37
χ^2	0.22	0.021	0.12	0.0011
R	0.98	0.998	0.96	0.9990

curves suggested homogeneous adsorption, although in the case of MB the curve shape was compatible with the possible occupation of two distinct sites of adsorption, namely, inside the channels of the fibrous hybrid clay minerals and on the grafted surface containing amine groups. In fact, the size of the channels allowed to be occupied by MB molecules, considering that MB molecules have a rigid structure constituted by interconnected benzene-like rings. The MY molecules showed a better mobility, due to the connection between the benzene rings by the azo group, but their size was larger and could not be inserted inside the pores. The size of the channels of both clay minerals and of MB and MY molecules are compared in Table 3 and Fig. S4. The behavior observed with the two fibrous clay minerals against adsorption of the two molecules dyes was different: MB was retained both in the natural and the functionalized clay mineral, functionalization was not a decisive factor. On the opposite, MY was not retained by the natural clay mineral but only by the treated solid, functionalization being a key factor.

The MB kinetic study showed that organofunctionalization did not alter the adsorption capacity (observed by the amount adsorbed, q_t = 2.49 mg/g). Indeed, in the initial times (until 5 min), Pal-APTES and Sep-APTES had lower adsorption capacities than the purified clay minerals, before this time all the samples reached the equilibrium and presented the same adsorption capacities. The presence of organic molecules on the surface may promote a negative effect on the final adsorption capacity for cationic dyes. This result is in agreement with the previously study for saponite clays grafted with amine groups in presence of CTA^+ ions (Marçal et al., 2015), the presence of well-distributed active sites favored the adsorption process; however, in excess these sites could hinder the adsorption. However, an opposite effect was observed for the anionic dye, the purified clay minerals were not able to adsorb the MY and the solids Pal-APTES and Sep-APTES showed q_t = 0.90 and 1.70 mg/g, respectively, proving that the adsorption of the anionic species is favored by the presence of amine groups on the surface of the fibrous clay minerals. To understand better this mechanism, the pH_{PZC} and the effect of the pH on the adsorption capacity were discussed.

Conflicting reports exist regarding the nature of adsorption of large molecules, such as dyes, onto Pal and Sep channels; two possible mechanisms have been proposed (Galán and Singer, 2011). The first mechanism assumed that the large organic molecules can fully exchange and replace cations and water molecules existing in the channels, a process which required an ordered transfer through the linear geometry of the confined channels along the 100 direction. The second mechanism considers that an efficient transport of large organic molecules and expulsion of the zeolitic water molecules through a fiber length was very hard; the insertion of large organic molecules actually showed many difficulties by steric hindrance, but the cationic environment and the excess of adsorbate in the solution promoted the mass transfer inside the fibrous clay mineral channels. In our case, only the cationic dye (MB) can be inserted inside the clay mineral channels, while the anionic/azo dye was adsorbed only in the surface due to its molecular size and chemical characteristics.

The yield of adsorption, defined as the percentage of dye existing in the solution that was adsorbed by the solid, was also evaluated under different dye concentrations (Fig. S5). For Pal-APTES, the affinity increased when the concentration of MY increased. However, the yield of adsorption of MB decreased drastically when the concentration was higher than 100 mg/dm^3. This gave good evidence that the adsorption of cationic MB occurred inside of Pal channels and the adsorption of MY was promoted by the grafting process (Fig. S5). To verify this assumption, adsorption was again studied, but using the original, ungrafted, purified fibrous clay; it was found that only MB was adsorbed. It has been previously reported that the adsorption of small dye molecules inside the channels of fibrous clay minerals was feasible from diluted solutions (Ruiz–Hitzky et al., 2013).

Maximum q_e values of 49.48 and 47.03 mg/g were achieved for Pal-APTES and 60.00 and 59.78 mg/g for Sep-APTES, for MB and MY, respectively (Table 4 and Fig. S5). Compared to other fibrous clay mineral adsorbents reported in the literature (Table 4), the adsorbents prepared with APTES had a very high affinity for both the anionic and cationic dyes, confirming the multifunctionality towards various species of these adsorbents.

3.2.2. Desorption and reuse

The uptake of the cationic dyes such as MB into clay minerals is generally attributed to a cation process, quantified by the cation exchange capacity (CEC). However, the fibrous clay minerals such as Pal and Sep show very low CEC values, merely from 10 to 20 mEq/100 g (Galán and Singer, 2011), and thus it is not possible to justify the adsorption process by cation exchange. For the fibrous aminofunctionalized clay minerals previously reported in the literature (Giles and Smith, 1974; Al–Futaisi et al., 2007; Dogan et al., 2007), adsorption generally occurred via hydrophobic interactions between the dye and the functionalized surface of the clay mineral. The desorption experiments were useful to confirm this point: when more apolar media were used as extraction solutions, desorption was favorable, while the presence of cationic species (concentrated sodium chloride solutions) did not increase the desorption capacity (Fig. 7). These results were opposite to those previously found for montmorillonite clay minerals with high

Table 3
Structural characteristics of the adsorbents and adsorbates used.

Pal channels (Å)	Sep channels (Å)	MB[a] (Å)	MY[a] (Å)
3.7 × 10.6[b]	3.7 × 6.4[b]	5.3 × 13.2[a]	6.1 × 17.3[a]
Effective internal diameter < 15 Å	Effective internal diameter < 15 Å	–	–
External pores > 15 Å	External pores > 15 Å	–	–

[a] Data calculated using Chem Sketch 12.0 ACD/Labs Software.
[b] Data obtained from literature (Galán and Singer, 2011).

Table 4
Maximum adsorption capacities (q_e) and comparison with other fibrous clays adsorbents.

Adsorbent	Modification agent	Dye adsorbed[a]	Maximum adsorption capacity, q_e (mg/g)	Reference
Pal-APTES	APTES	MB	49.48	This work
		MY	47.03	
Sep-APTES	APTES	MB	60.00	
		MY	59.78	
Palygorskite	–	MB	48	Özdemir et al. (2006)
		CV	33	
Palygorskite	APTES	RR	16.514	Xue et al. (2011)
		RBK	16.582	
		RKG	16.119	
Sepiolite	–	MV	7.34–10.60	
		MB	52.13–87.31	
		MV	Not shown	Dogan et al. (2007)
		MB		

[a] MB: methylene blue; MY: metanil yellow; CV: crystal violet; RR: reactive red 3BS; RBK: reactive blue KE-R; RKG: reactive black GR; MV: methyl violet.

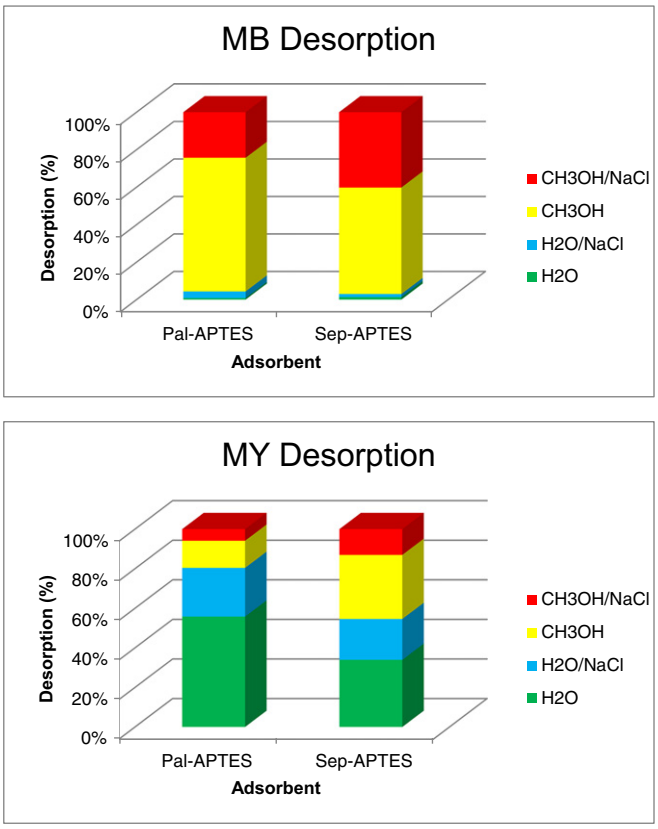

Fig. 7. Desorption of MB and MY dyes from the hybrid adsorbents.

CEC (Berhane et al., 2015), where cation exchange was the main adsorption mechanism. For MB, the methanol solution of sodium chloride was the best extraction medium, but for the anionic dye, maximum desorption was observed for the aqueous solutions. This is a key point regarding the regeneration of the adsorbents from a Green Chemistry viewpoint. Desorption experiments proved the higher affinity of cationic MB for the aminofunctionalized clay minerals; however, the major contribution to the adsorption mechanism occurred via hydrophobic interaction and/or hydrogen bonds (Fig. S6). As previously discussed (Ruiz–Hitzky et al., 2013), due to the natural tendency of MB to form molecular aggregates, it cannot be inserted inside the Sep channels from a concentrated medium ($>10^{-3}$ mol/dm^3), but it can be adsorbed inside the fibrous channels from diluted solutions. In the equilibrium experiments, the higher efficiencies were obtained for concentrations lower than 100 mg/g when using Pal, and 600 mg/g when using Sep (Giles and Smith, 1974; Al–Futaisi et al., 2007; Dogan et al., 2007). Thus, the insertion of the cationic dye inside the clay mineral pores made difficult further desorption.

Evaluation of adsorbent reusing is a very important factor, although it is scarcely studied, as generally only adsorption experiments are carried out. The solids were washed after desorption experiments, dried and used in new adsorption experiments. In the case of MB, comparable efficiencies were obtained in the second cycle for both adsorbents, while for MY a strong decrease in the adsorption capacity was observed, especially when using hybrid Pal (Fig. S7). This decrease in the adsorption ability may be due to the presence of remaining adsorbed MY, not removed by washing; so, the main difference could be tentatively related to the easier washing of cationic MB than anionic MY from the surface of the hybrid adsorbents. The physicochemical characterization of the solids by PXRD and FTIR did not show significant changes after the adsorption-desorption cycle, confirming their high stability and their reuse ability.

3.2.3. pH effect

The batch equilibrium method was applied to determine the pH_{PZC} of the purified fibrous clay minerals and the hybrid materials used here as adsorbents. pH_{final} readings were plotted as a function of $pH_{initial}$ in Fig. 8. The pH_{final} value of the resulting *plateau* was assigned to the pH at which there was not net OH^- or H^+ adsorption. At this pH, the difference between the initial and the final $[H^+]$ or $[OH^-]$ is zero. The calculated pH_{PZC} were 3.9 and 7.2 for Pal and Sep, respectively; and 9.8 for both hybrid materials. After grafting of APTES, the presence of basic NH_2 groups changed the charge of the surface to basic character, as suggested by the pH_{PZC} values obtained for the two hybrid materials.

Dogan et al. (2007) reported pH_{PZC} close to 6.7 for fibrous clay minerals. At lower pH values, the association of anionic dyes such as MY with the surface of sepiolite, positively charged by the presence of Clay-OH_2^+ groups, can take place easily. However, the increase in pH charges negatively the clay surface and the interaction with anionic dyes is no longer favored. Thus, at pH above the pH_{PZC} of the adsorbent, i.e., 6.7, the adsorbent surface will be more easily associated to cationic dyes.

pH is an important factor controlling the extent of dye adsorption in aqueous suspensions of layered or fibrous clay minerals (Alkan et al., 2005). Adsorption generally depends on the electrokinetic behavior of the solid, as determined by the amount of H^+/OH^- adsorbed on the clay surface. Alkan et al. (2005) reported that in natural and aminofunctionalized fibrous clay minerals the surface is positively charged at low pH where reaction (Fig. 9-A) predominates, and is negatively charged at higher pH when reaction (Fig. 9-B) takes over. We observed the same effect after grafting, as the $-NH_2$ groups could be protonated generating $-NH_3^+$ cations and the residual hydroxyl surfaces generating negative charges induced by the OH^- ions from the aqueous solution.

The amounts of MB and MY adsorbed by the solids changed drastically as a function of pH, showing an opposite trend (Fig. 10). In the case of MB, the adsorption capacity decreased upon increasing the pH solution, probably by the progressive deprotonation of the $-NH_3^+$ groups, which may decrease the electrostatic attraction between the surface and the dye anions (Selvam et al., 2001; Alkan et al., 2005; Dogan et al., 2007). Very similar results have been also reported for the adsorption of anionic dyes on ammonium-functionalized MCM-41 (Qin et al., 2009). The opposite trend was observed for the adsorption of MY, which can be explained in a similar way.

3.2.4. Real dyestuff wastewater adsorption proof

A simple qualitative test of adsorption was carried out with a real effluent from a textile industry before and after biological treatment. The

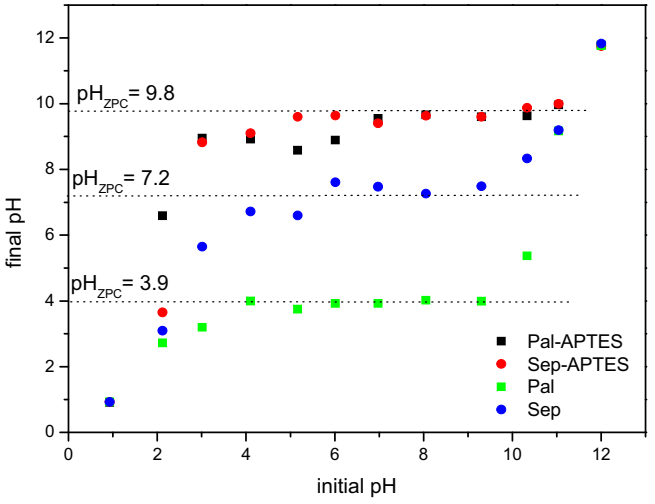

Fig. 8. pH_{PZC} obtained from batch equilibrium method of the purified fibrous clay minerals (Pal and Sep) and hybrid materials (Pal-APTES and Sep-APTES).

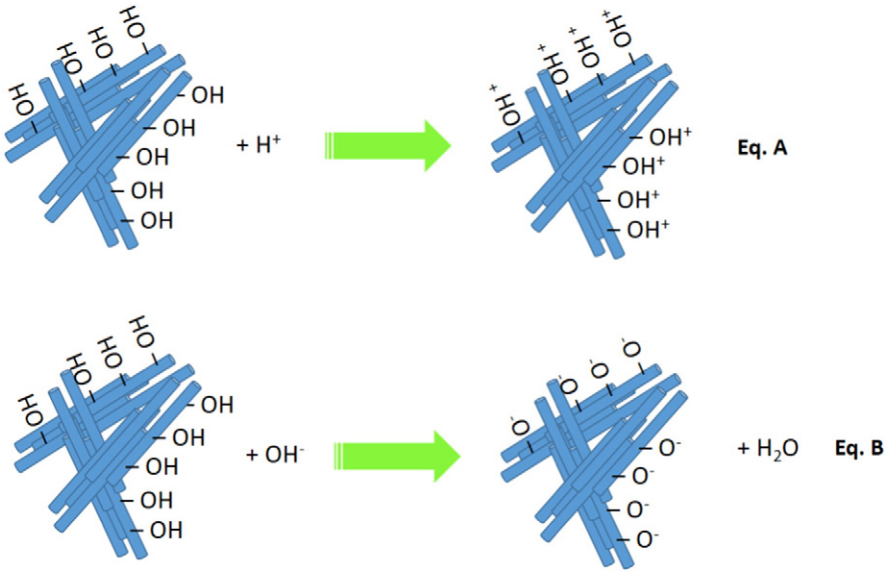

Fig. 9. Schematic representation of charges generated on clay mineral surfaces at different pH.

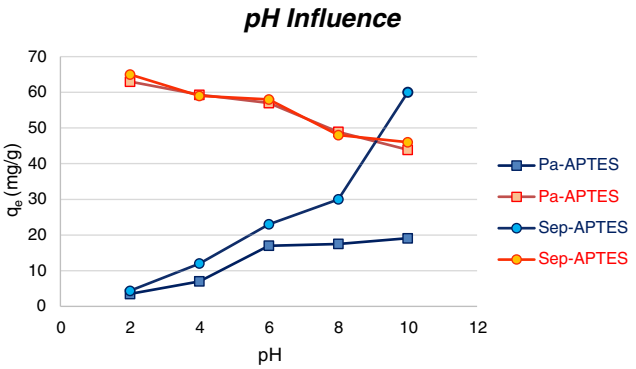

Fig. 10. Adsorption capacity of Pal-APTES and Sep-APTES as a function of pH.

effluent contained a complex mixture of dyes and sulfate, nitrate, carbonate and chloride, among other species. Both Pal-APTES and Sep-APTES adsorbents were effective for adsorption (color removal higher than 50%) and desorption cycles under real conditions without change of pH.

Wastewater A was composed of a complex mixture; the band at 256 nm was very intense proving the presence of high amount of contaminants. However, the band at 256 nm for wastewater B had a lower intensity, as the amount of contaminants after the biological treatment was lower. The color of the wastewater before and after centrifugation can be seen in Fig. 11.

In the case of wastewater A (before biological treatment), similar efficiencies were observed for both materials; the highest removal efficiency was obtained for Sep-APTES solid, 55% after 60 min, and 48% when using Pal-APTES as adsorbent (Fig. 12). The lower contaminant removal by Pal-APTES was assigned to the lower specific surface area for the hybrid material based on palygorskite. The important conclusion was the possibility of using hybrid-fibrous clay minerals as efficient adsorbents for real wastewaters. The same profile was obtained for wastewater B (after biological treatment) under lower concentrations of the contaminants, confirming the efficiency of both adsorbents (Fig. 13). It is very important to remark that the adsorption experiments were carried out without any previously preparation or dilution, only filtration. The adsorption process occurred with high efficiency, without loss of the adsorption capacity, using simple conditions without changes in pH or temperature, and for sample A without any other primary treatments (for sample B, as indicated, biological treatment was carried out).

Although the optimum adsorption parameters deduced for the model dyes (MB and MY) study were applied, the results for the real textile effluent were not consistent in some cases, probably because each wastewater was composed of a complex admixture of various contaminants. Adsorption was efficient, but the number of contaminants such as another cationic or anionic species made the adsorption and removal processes more complicated to understand. Thus, more research

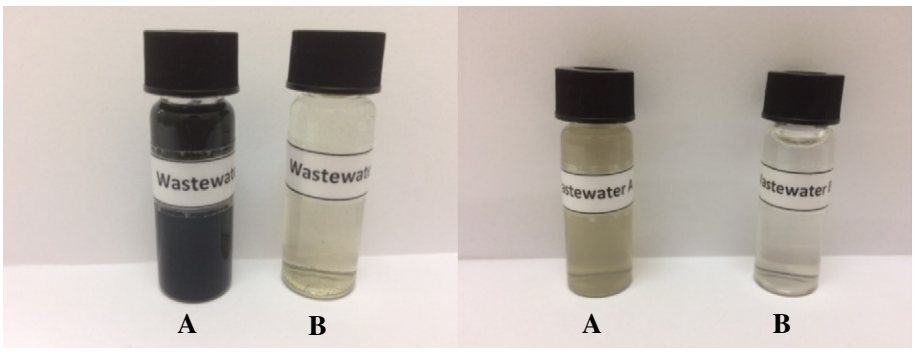

Fig. 11. Photograph of initial wastewater samples (A: without biological treatment and B: post-biological treatment, respectively), left: non-centrifuged and right: centrifuged.

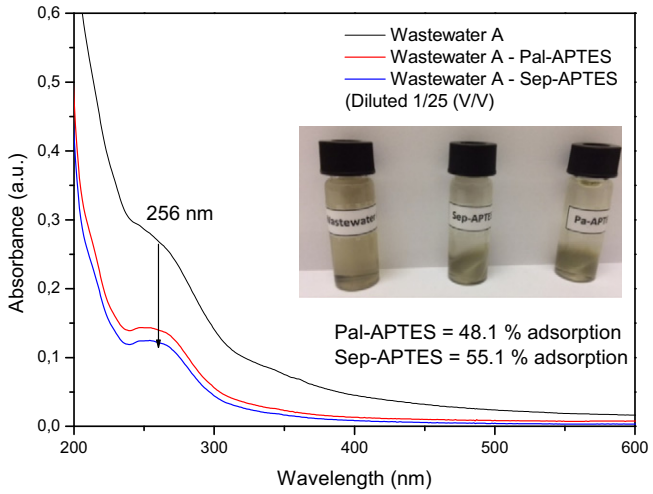

Fig. 12. UV–vis absorption spectra of wastewater A before and after adsorption experiments.

should be carried out for understanding the complexity of the system before further application.

4. Conclusions

Surface silanization of fibrous clay minerals by APTES was effective, the infrared spectra of the treated solids displayed the characteristic bands of amine groups (3350 and 1610 cm^{-1}) confirming that the alkoxide was grafted onto the fibrous clay minerals. The presence of the typical reflections of clay minerals in the PXRD evidenced that solids maintained unaltered after grafting.

Both fibrous hybrid clay minerals were effectively used as adsorbents for removing cationic (MB) and anionic (MY) dyes. The time required for reaching the equilibrium was shorter than 30 min for both adsorbents. The pseudo-second-order kinetic model efficiently described the kinetics of the adsorption of dyes. MB and MY adsorption occurred on the surface of the hybrid fibrous clay minerals and in the specific case of MB could occur also inside of the channels. In both cases, grafting of the surface drastically increased the adsorption capacity, mainly for the anionic species. The adsorbents could be efficiently reused in a second adsorption cycle after desorption. All the results revealed the multifunctionality of hybrid fibrous clay minerals as dye adsorbents. Results for real textile effluents showed that adsorption was

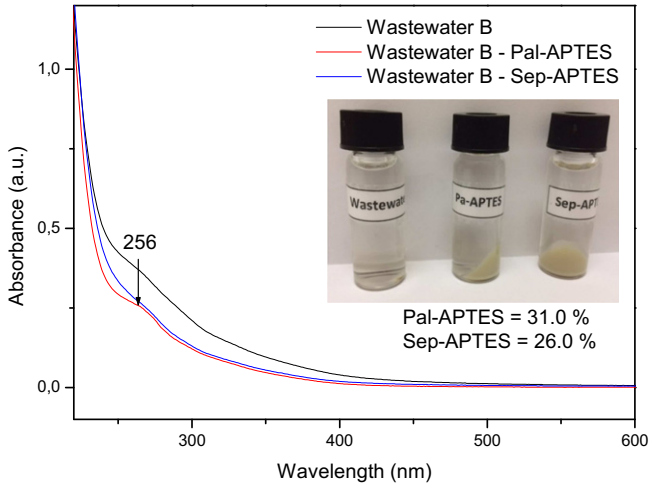

Fig. 13. UV–vis absorption spectra of wastewater B before and after adsorption experiments.

efficient for the two samples evaluated, but due to the higher number of contaminants present in the wastewaters, the adsorption and removal processes were very complex and more research should be carried out for understanding them before application.

Acknowledgments

This work was carried out in the frame of a Spain–Brazil Interuniversity Cooperation Grant, funded by MEC (PHBP14/00003) and CAPES (317/15), and a Cooperation Grant Universidad de Salamanca–FAPESP (2013/50216–0). Spanish authors thank additional financial support from Ministerio de Economía y Competitividad (grant MAT2013–47811–C2–R). The Brazilian group thanks support from Brazilian Research funding agency FAPESP (2013/09149–7 and 2013/19523–3). E.H. de Faria and K.J. Ciuffi thank CNPq Grants (311767/2015–0 and 305398/2015–6, respectively).

Appendix A. Supplementary data

Supplementary data to this article can be found online at doi:10.1016/j.clay.2016.10.022.

References

Afkhami, A., Bagheri, H., Madrakian, T., 2011. Alumina nanoparticles grafted with functional groups as a new adsorbent in efficient removal of formaldehyde from water samples. Desalination 281, 151–158.
Al–Futaisi, A., Jamrah, A., Al–Hanai, R., 2007. Aspects of cationic dye molecule adsorption to palygorskite. Desalination 214, 327–342.
Alkan, M., Çerlikçapa, S., Demirbas, Ö., Dogan, M., 2005. Removal of reactive blue 221 and acid blue 62 anionic dyes from aqueous solutions by sepiolite. Dyes Pigments 6, 251–259.
Anandkumar, J., Mandal, B., 2011. Adsorption of chromium(VI) and rhodamine B by surface modified tannery waste: kinetic, mechanistic and thermodynamic studies. J. Hazard. Mater. 186, 1088–1096.
Barbosa, L.V., Marçal, L., Nassar, E.J., Ciuffi, K.J., Calefi, P.S., Vicente, M.A., Trujillano, R., Rives, V., Gil, A., Korili, S., de Faria, E.H., 2015. Kaolinite–titanium oxide nanocomposites prepared via sol–gel as heterogeneous photocatalysts for dyes degradation. Catal. Today 246, 133–142.
Berhane, T.M., Levy, J., Krekeler, M.P.S., Danielson, N.D., Stalcup, A., 2015. Sorption–desorption of carbamazepine by palygorskite–montmorillonite (PM) filter medium. J. Hazard. Mater. 282, 183–193.
Bezerra, D.P., da Silva, F.W.M., de Moura, P.A.S., Sousa, A.G.S., Vieira, R.S., Rodriguez–Castellon, E., Azevedo, D.C.S., 2014. CO_2 adsorption in amine–grafted zeolite 13X. Appl. Surf. Sci. 314, 314–321.
Bizaia, N., de Faria, E.H., Ricci, G.P., Calefi, P.S., Nassar, E.J., Castro, K.A.D.F., Nakagaki, S., Ciuffi, K.J., Trujillano, R., Vicente, M.A., Gil, A., Korili, S.A., 2009. Porphyrin-kaolinite as efficient catalyst for oxidation reactions. ACS Appl. Mater. Interfaces 1, 2667–2678.
Cagatay, M.N., 1990. Palygorskite in the Eocene rocks of the Dammam dome, Saudi Arabia. Clay Clay Miner. 38, 299–307.
de Faria, E.H., Lima, O.J., Ciuffi, K.J., Nassar, E.J., Vicente, M.A., Trujillano, R., Calefi, P.S., 2009. Hybrid materials prepared by interlayer functionalization of kaolinite with pyridine–carboxylic acids. J. Colloid Interface Sci. 335, 210–215.
Demirbas, E., Kobya, M., Sulak, M.T., 2008. Adsorption kinetics of a basic dye from aqueous solutions onto apricot stone activated carbon. Bioresour. Technol. 99, 5368–5373.
Dogan, M., Özdemir, Y., Alkan, M., 2007. Adsorption kinetics and mechanism of cationic methyl violet and methylene blue dyes onto sepiolite. Dyes Pigments 75, 701–713.
El–Rehim, H.A.A., Hegazy, E.A., Diaa, D.A., 2012. Photo–catalytic degradation of Metanil Yellow dye using TiO_2 immobilized into polyvinyl alcohol/acrylic acid microgels prepared by ionizing radiation. React. Funct. Polym. 72, 823–831.
Frost, R.L., Mendelovici, E., 2006. Modification of fibrous silicates surfaces with organic derivatives: an infrared spectroscopic study. J. Colloid Interface Sci. 294, 47–52.
Frost, R.L., Xi, Y., He, H., 2010. Synthesis, characterization of palygorskite supported zero–valent iron and its application for methylene blue adsorption. J. Colloid Interface Sci. 341, 153–161.
Developments in clay science. In: Galán, E., Singer, A. (Eds.), Developments in Palygorskite–Sepiolite ResearchA New Outlook on These Nanomaterials vol. 3. Elsevier.
Giles, C.H., Smith, D., 1974. A general treatment and classification of the solute adsorption isotherm. J. Colloid Interface Sci. 47, 755–765.
Gupta, V.K., Jain, R., Varshney, S., 2007. Electrochemical removal of the hazardous dye Reactofix Red 3 BFN from industrial effluents. J. Colloid Interface Sci. 312, 292–296.
Ho, Y., Ofomaja, A.E., 2006. Pseudo–second–order model for lead ion sorption from aqueous solutions onto palm kernel fiber. J. Hazard. Mater. 129, 137–142.
Jain, A.K., Gupta, V.K., Bhatnagar, A., Suhas, T.L., 2003. Utilization of industrial waste products as adsorbents for the removal of dyes. J. Hazard. Mater. 101, 31–42.
Lagergren, S., 1898. About the theory of so–called adsorption of soluble substances. Kungliga Svenska Vetenskapsakademiens Handlingar 24, 1–39.

Letaief, S., Grant, S., Detellier, C., 2011. Phenol acetylation under mild conditions catalyzed by gold nanoparticles supported on functional pre–acidified sepiolite. Appl. Clay Sci. 53, 236–243.
Linneen, N.N., Pfeffer, R., Lin, Y.S., 2014. CO_2 adsorption performance for amine grafted particulate silica aerogels. Chem. Eng. J. 254, 190–197.
Machado, G.S., Ucoski, G.M., de Lima, O.J., Ciuffi, K.J., Wypych, F., Nakagaki, S., 2013. Cationic and anionic metalloporphyrins simultaneously immobilized onto raw halloysite nanoscrolls catalyze oxidation reactions. Appl. Catal. A Gen. 460–461, 124–131.
Marçal, L., de Faria, E.H., Nassar, E.J., Trujillano, R., Martín, N., Vicente, M.A., Rives, V., Gil, A., Korili, S.A., Ciuffi, K.J., 2015. Organically modified saponites: SAXS study of swelling and application in caffeine removal. ACS Appl. Mater. Interfaces 7, 10853–10862.
Matusik, J., Wścisło, A., 2014. Enhanced heavy metal adsorption on functionalized nanotubular halloysite interlayer grafted with aminoalcohols. Appl. Clay Sci. 100, 50–59.
Nagaraja, T.N., Desirajut, T., 1993. Effects of chronic consumption of metanil yellow by developing and adult rats on brain regional levels of noradrenaline, dopamine and serotonin, on acetylcholine esterase activity and operant conditioning. Food Chem. Toxicol. 31, 41–44.
Neaman, A., Singer, A., 2000. Rheological properties of aqueous solution of palygorskite. Soil Sci. Soc. Am. J. 64, 427–436.
Önal, M., Sarikaya, Y., 2009. Some physicochemical properties of a clay containing smectite and palygorskite. Appl. Clay Sci. 44, 161–165.
Özdemir, Y., Dogan, M., Alkan, M., 2006. Adsorption of cationic dyes from aqueous solutions by sepiolite. Microporous Mesoporous Mater. 96, 419–427.
Ozer, D., Dursun, G., Ozer, A., 2007. Methylene blue adsorption from aqueous solution by dehydrated peanut hull. J. Hazard. Mater. 144, 171–179.
Qin, Q., Ma, J., Liu, K., 2009. Adsorption of anionic dyes on ammonium-functionalized MCM-41. J. Hazard. Mater. 162, 133–139.
Ruiz–Hitzky, E., Darder, M., Fernandes, F.M., 2013. Fibrous clays based bionanocomposites. Prog. Polym. Sci. 38, 1392–1414.
Saha, S., Sarkar, P., 2012. Arsenic remediation from drinking water by synthesized nano–alumina dispersed in chitosan–grafted polyacrylamide. J. Hazard. Mater. 227–228, 68–78.
Sahoo, C., Gupta, A.K., 2012. Optimization of photocatalytic degradation of methyl blue using silver ion doped titanium dioxide by combination of experimental design and response surface approach. J. Hazard. Mater. 215–216, 302–310.
Selvam, P., Bhatia, S.K., Sonwane, C.G., 2001. Recent advances in processing and characterization of periodic mesoporous MCM-41 silicate molecular sieves. Ind. Eng. Chem. Res. 40, 3237–3261.
Sing, K.S.W., Everett, D.H., Haul, R.A.W., Moscou, L., Pierotti, R.A., Rouquerol, J., Siemieniewska, T., 1985. Reporting physisorption data for gas/solid systems with special reference to the determination of surface area and porosity. Pure Appl. Chem. 57, 603–619.
Tiozzo, C., Bisio, C., Carniato, F., Guidotti, M., 2014. Grafted non–ordered niobium–silica materials: versatile catalysts for the selective epoxidation of various unsaturated fine chemicals. Catal. Today 235, 49–57.
Tonlé, I.K., Diaco, T., Ngameni, E., Detellier, C., 2007. Nanohybrid kaolinite–based materials obtained from the interlayer grafting of 3–aminopropyltriethoxysilane and their potential use as electrochemical sensors. Chem. Mater. 19, 6629–6636.
Wayde, B.P., Martens, N., Frost, R.L., 2011. Organosilane grafted acid–activated beidellite clay for the removal of non–ionic alachlor and anionic imazaquin. Appl. Surf. Sci. 257, 5552–5558.
Xue, A., Zhou, S., Zhao, Y., Lu, X., Han, P., 2011. Effective NH_2–grafting on attapulgite surfaces for adsorption of reactive dyes. J. Hazard. Mater. 194, 7–14.